H1prelim-08-036 Submitted to

34th International Conference on High Energy Physics, ICHEP2008, 30th July - 5th August, Philadelphia

Abstract: **xx-xxx**

Parallel Session **QCD/Lattice**

Electronic Access: www-h1.desy.de/h1/www/publications/conf/conf_list.html

Study of Multiple Interactions in photoproduction at HERA (version of July 22, 2008)

H1 Collaboration

Abstract

Photoproduction data of HERA-I are analysed by requiring dijets with transverse momenta of at least 5 GeV. The two jets define in azimuth a towards region (leading jet) and an away region (2nd jet) and transverse regions between them. The charged particle multiplicity is measured in these regions as a function of the variables x_γ and P_T (leading jet). PYTHIA predictions including contributions of multi-parton interactions are able to describe the measurement, whereas without them they lie below the measurements, especially at low x_γ, the region of enhanced contributions from the resolved photon.

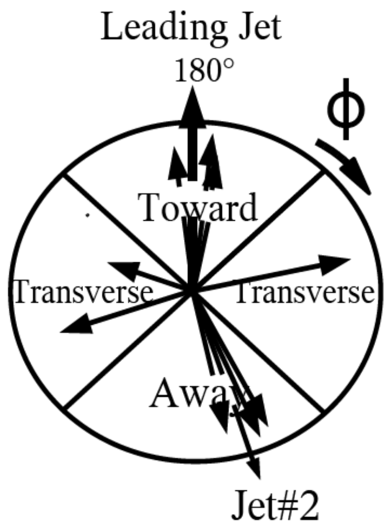

Figure 1: *Toward, away and transverse regions defined. In the toward region the leading jet is always at $\phi = 180^o$ and is the reference to define the other regions.*

1 Introduction

In quasi-real photoproduction ($Q^2 \sim 0$) the photon has a point-like as well as a hadronic (resolved) component. Measurements in photoproduction at HERA have the advantage that the transition from a point-like photon towards a resolved photon can be studied in detail as function of the variable x_γ. Multi-parton interactions are expected within the model of [1, 2] for resolved photons ($x_\gamma < 1$) but not for the point-like photons which have $x_\gamma \sim 1$. This fact was already used for multi-parton studies at HERA in [3], where it was shown that jet production and energy flow are well described when including multi-parton interactions.

In the photoproduction of dijets at HERA the underlying event can be studied in a fashion similar to the studies done at the TeVatron [4]. The underlying event is here defined as everything in addition to the lowest order process, here dijet production. The underlying event will consist of contributions coming from higher order QCD radiation, simulated by parton showers, hadronisation and also of multi-parton interactions. This multi-parton interactions take place when the density of partons in the colliding beams is large enough that more than one interaction happens within one collision.

Multi-parton interactions have been required to describe the transverse momentum and particle multiplicity distributions in a region transverse to the jets at the TeVatron, see Fig.1. Here an analysis is presented which follows closely this analysis to investigate the effect of the underlying event and multi-parton interactions in photoproduction at HERA.

2 Monte Carlo Model

The full hadronic final state is simulated with the PYTHIA Monte Carlo event generator including the lowest order matrix element processes for direct and resolved photoproduction together

Description	Used	Default
MSTP(93)	5	1
PARP(82)	1.2	2
PARP(99)	0.6	1
PARP(85)	0.33 (1.)	0.9
PARP(86)	0.66 (1.)	0.95
PARP(83)	0.5	0.5
PARP(84)	0.4	0.4
PARP(89)	1800	1800
PARP(90)	0.25	0.16

Table 1: The relevant parameters for the PYTHIA simulation.

with parton showers to simulate higher order QCD corrections and hadronisation. In PYTHIA the Lund String fragmentation is implemented.

PYTHIA includes multi-parton interactions (MPI): several partons of the proton can interact with several partons of the resolved photon. The details of the multi-parton interaction model is described in [1,2]. For the photoproduction case only a simple version of this model is available. A similar model was used also to describe the TeVatron measurements.

When multi-parton interactions occur, the formation of colour neutral strings or clusters is far from trivial as colour exchange might happen between the different interactions. In the Lund String model long strings will produce a larger multiplicity of hadrons compared to short strings. The transverse energy, however, is mainly driven by the high-p_t hard scattering process. Thus the particle multiplicity together with the average transverse momentum distribution yields non-trivial information about the colour structure of jet events.

Events are generated with the PYTHIA Monte Carlo event generator with multi-parton interactions switched on. The proton pdf was CTEQ6L [5] and the photon pdf was SaS1D [6]. All generated events are passed through the full simulation of the H1 apparatus and are reconstructed using the same program chain as for the data.

The final results of the measurement are then compared with predictions from PYTHIA at hadron level. The different settings are given in Tab.1. It was explicitly checked that same set of parameters in PYTHIA 6.2 and PYTHIA 6.4 give the same results. The measurements are compared with Monte Carlo simulations with and without multi-parton interactions and with different options for the colour configuration, as given by the parameter PARP(85), PARP(86) for short (PARP(85)=PARP(86)=1) and long string (PARP(85)=0.33, PARP(86)=0.66) configurations.

Event Selection

Data are recorded in the running period 1999-2000, $\mathcal{L} = 48\ pb^{-1}$, where HERA was operated with positron and proton beams of $E_e = 26.7$ GeV and $E_p = 920$ GeV respectively giving a center-of-mass energy of $\sqrt{s} = 318$ GeV.

Photoproduction events are selected by requiring a signal in the electron tagger which has acceptance in the inelasticity range $0.3 < y < 0.65$, which results in $Q^2 < 0.01$ GeV^2. The reconstructed primary vertex position, $z-$vertex, has to be within 35 cm of the nominal one.

Jets are selected with the inclusive k_t-jet algorithm using as input combined objects, i.e. four-vectors objects, where information from track and/or cluster is combined. At least two jets are required with $P_T^{jet} > 5$ GeV within a pseudorapidity range in the laboratory frame of $-1.5 < \eta_{lab} < 1.5$. The jet with the highest P_T^{jet} defines the leading jet, Jet_1. From the jets the value x_γ is calculated:

$$x_\gamma = \frac{\sum_{h \in Jet_1}(E - P_z) + \sum_{h \in Jet_2}(E - P_z)}{\sum_h (E - P_z)} \tag{1}$$

Tracks are selected having a $P_T^{track} > 150$ MeV within $|\eta| < 1.5$. The difference in azimuthal angle $\Delta\phi = \phi_{Jet_1} - \phi_i$ with i running over all charged particles satisfying the above cuts, is calculated, with the leading jet set to $\phi = 180^o$.

Four different regions in azimuth with respect to the leading jet are defined, see Fig.1:

- the toward region (including the leading jet) with $120^o < \Delta\phi < 240^o$
- the away region with $300^o < \Delta\phi < 60^o$
- the transverse region with $60^o < \Delta\phi < 120^o$ and $240^o < \Delta\phi < 300^o$

In the transverse region the scalar sum of the transverse momenta $E_t^{sum} = \sum_i^{tracks} P_T^i$ is calculated and the region with the higher E_t^{sum} is defined as the *high activity* region. The direction of ϕ is defined such, that the *high activity* is always $240^o < \Delta\phi < 300^o$.

The average multiplicity distributions are measured as a function of the angular difference $\Delta\phi$ and as a function of the leading jet transverse momentum P_T^{jet} for the four different regions in $\Delta\phi$. The distributions are corrected to charged stable hadrons level using an iterative Bayes unfolding method (see [7]).

Systematic Uncertainties

In this section, the systematic uncertainties associated with the measurement of photoproduction of dijets are discussed. The uncertainties on the signal extraction are determined by varying the following quantities:

- ± 2 % for the track finding in CJC, ± 1 % for the vertex reconstruction using central tracks and ± 1.5 % for uncertainties in the simulation of nuclear interaction resulting in a ± 2.7 % independent and uncorrelated uncertainty independent of P_T and η of the charged tracks.
- ± 2 % of the hadronic energy scale of the calorimeter for the construction of combined objects.

- In case the difference in E_t^{sum} between the high and low activity transverse region is less than 160 MeV the probability to misidentify the high and low activity regions is estimated to be 10%.

- $2 - 4$ % uncertainty from the limited statistics used in the unfolding.

The individual effects of the above experimental uncertainties are combined in quadrature, yielding a total uncertainty of $\sim 3\%$ on the signal expectation. The largest contributions to this uncertainty arise from systematics attributed to tracking (2.7% nearly constant over all regions and phase space) and to the hadronic energy scale (0.5% in the toward and away regions and $0.5\% - 1.5\%$ in the transverse regions).

3 Results

The results shown here are always shown for two regions in x_γ: a resolved photon enriched region with $x_\gamma < 0.7$ and a point-like photon enriched region with $x_\gamma > 0.7$. The average track multiplicity as a function of $\Delta\phi$ is shown in Fig. 2 for the two regions in x_γ. One can see clearly the leading jet which is by definition at $\Delta\phi \sim 180^o$, the second jet at $\Delta\phi \sim 0^o$ and $\Delta\phi \sim 360^o$ as well as contributions of a third jet which is in the region of $\Delta\phi > 240^o$. The data are compared to predictions of PYTHIA. In the large x_γ region the effect of multi-parton interaction is very small, in the region of $x_\gamma < 0.7$ the inclusion of multi-parton interaction clearly improves the description in the transverse regions as well as in the toward and away regions where it contributes as a pedestal to the track multiplicity.

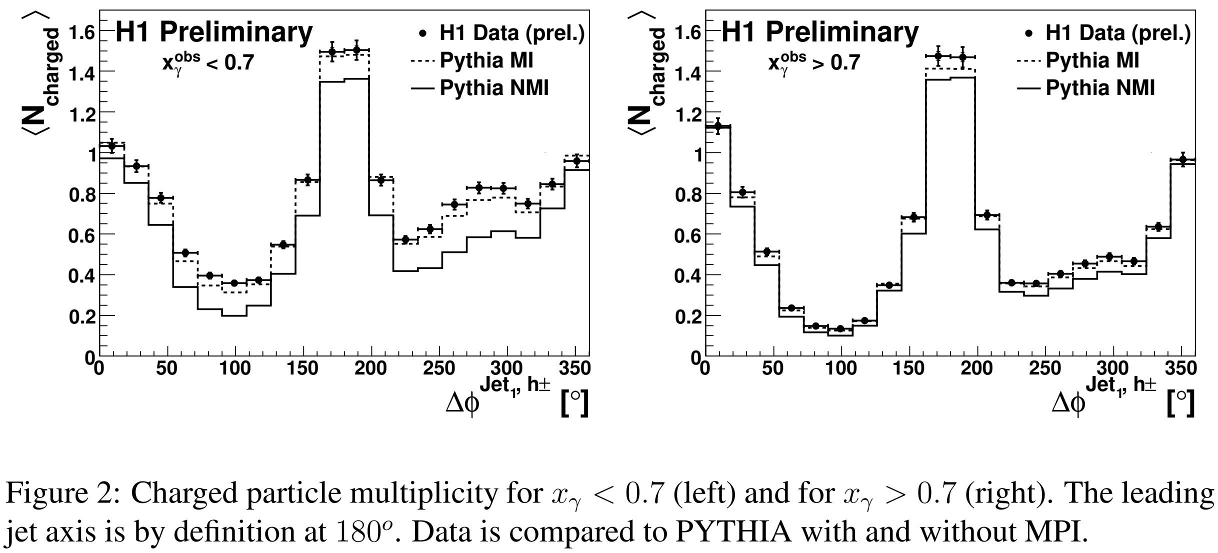

Figure 2: Charged particle multiplicity for $x_\gamma < 0.7$ (left) and for $x_\gamma > 0.7$ (right). The leading jet axis is by definition at 180^o. Data is compared to PYTHIA with and without MPI.

In Fig. 3 the average charge particle multiplicity is shown for the two regions in x_γ for the toward and away regions. In general the average track multiplicity rises with increasing $P_T^{Jet_1}$ from around 4-5 particles at $P_T^{Jet_1} \sim 5$ GeV to around 7 particles $P_T^{Jet_1} > 15$ GeV also depending on x_γ. In the region of $x_\gamma > 0.7$ the measurements are reasonably well described with a simulation containing only one hard interaction together with parton showers and hadronisation, whereas in the region $x_\gamma < 0.7$ this is clearly not enough, especially at the lower values of $P_T^{Jet_1}$. Including multi-parton interactions brings the prediction in good agreement with the measurement.

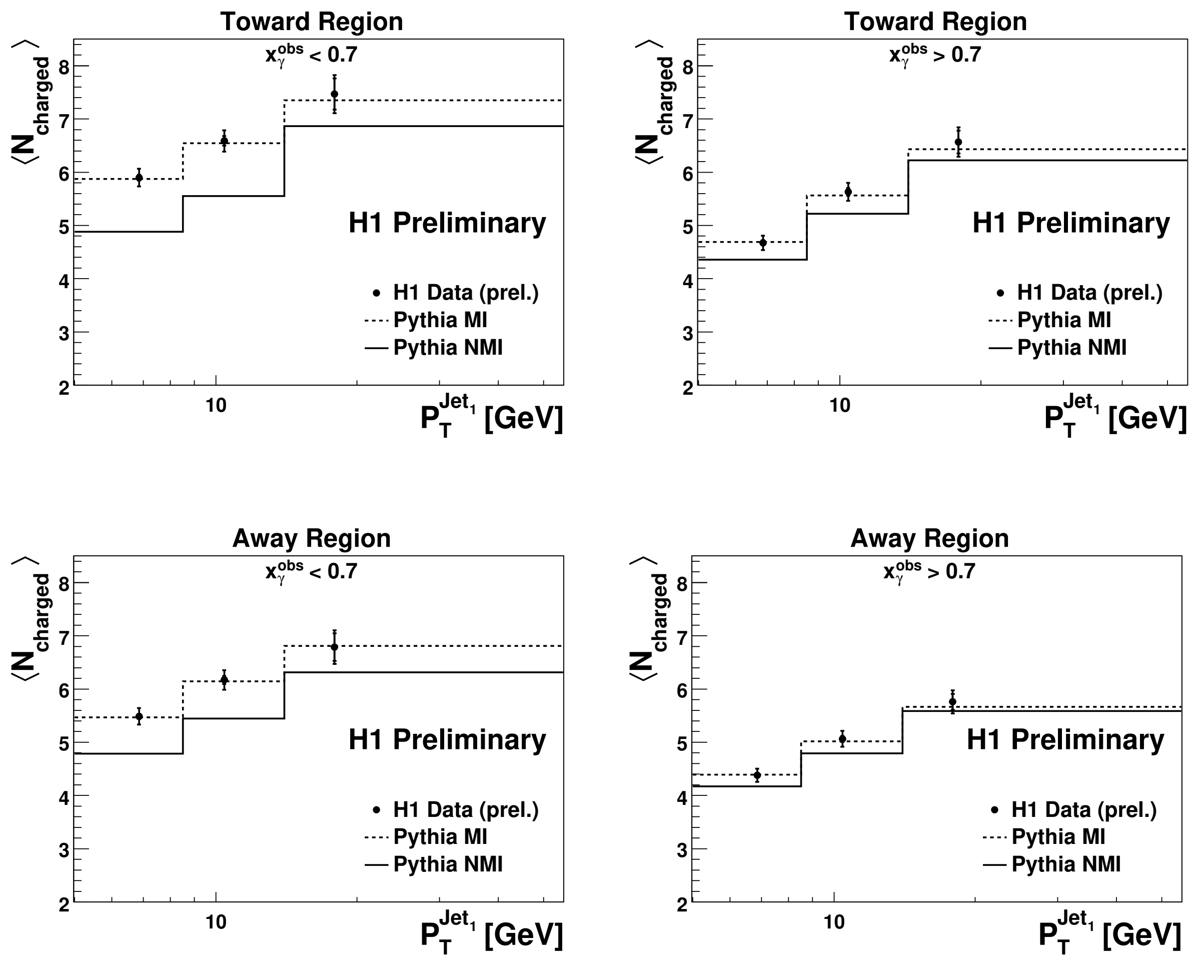

Figure 3: Charged particle multiplicity for $x_\gamma < 0.7$ (left) and for $x_\gamma > 0.7$ (right). The toward regions, upper plots, contain the leading jet whereas the second jet is usually found in the away regions, down. Data is compared to PYTHIA with and without MPI.

In Fig. 4 the average charged particle multiplicity in the traverse region is shown for the two regions in x_γ. Here the average charged particle multiplicity ranges between 0.5 to 2.5 particles depending on x_γ and $P_T^{Jet_1}$. In the region of $x_\gamma > 0.7$ the measurements are again reasonably well described without including MPI, whereas the region of $x_\gamma < 0.7$ requires a larger average multiplicity than predicted from a simulation without MPI. The simulation including MPI gives a reasonable description of the measurement over the full phase space region.

It is interesting to investigate whether the measurements can also be described by including more higher order QCD radiation, which can be approximately simulated by changing the upper scale in the initial and final state parton shower simulation, PS. Setting the upper scale to four times the scale of the hard scattering process results in harder partons from the parton shower.

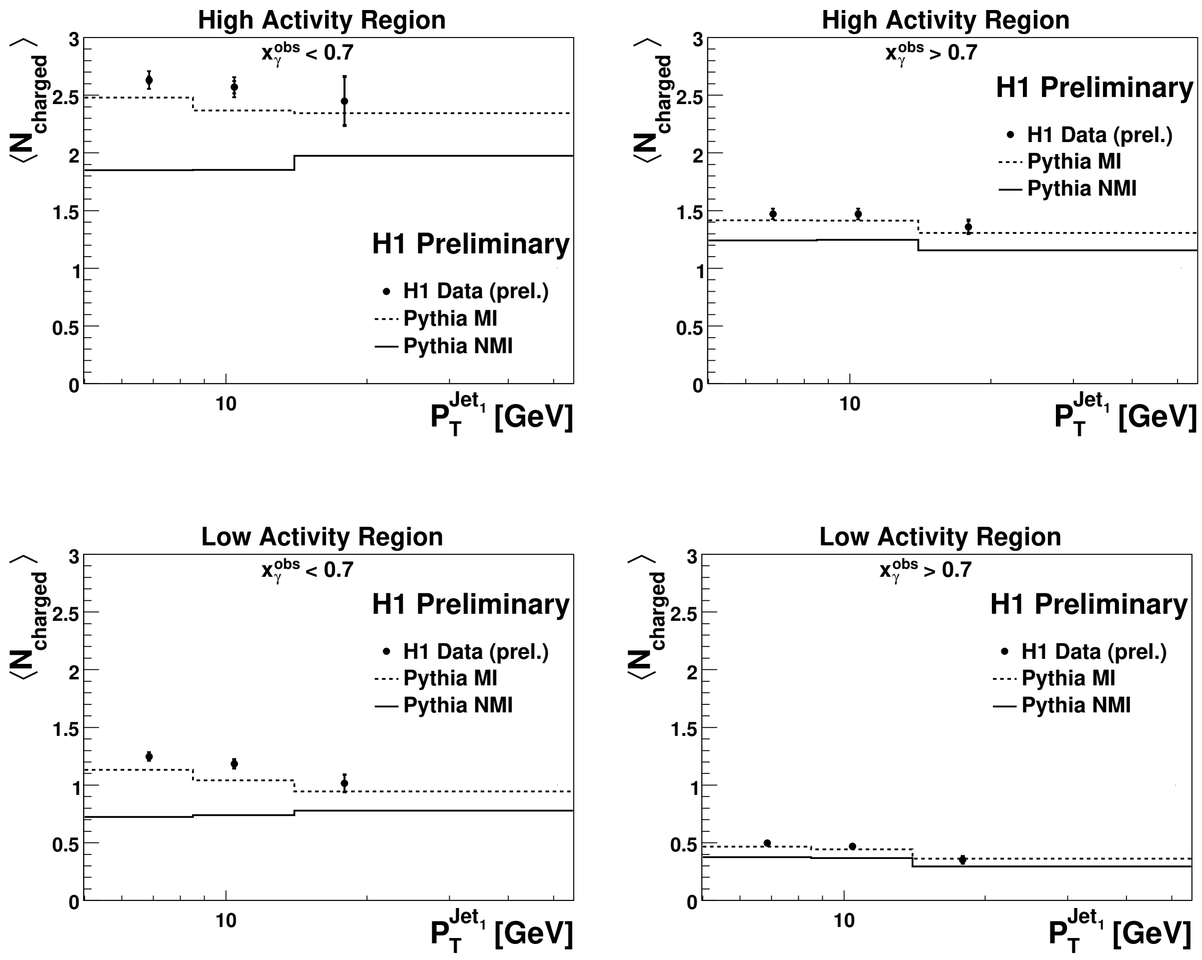

Figure 4: Charged particle multiplicity for $x_\gamma < 0.7$ (left) and for $x_\gamma > 0.7$ (right). The transverse high activity regions, upper plots, are defined as the transverse region with a higher E_t^{sum} compared to the low activity regions, down. Data is compared to PYTHIA with and without MPI.

The comparison of a simulation with an upper scale four times the hard scattering scale and a simulation with this upper scale set to the hard scattering is shown in Fig. 5. Only in the high activity region a effect of the parton shower can be seen, but this is not enough to bring the simulation close to the measurement, indicating that higher order contributions cannot account for the high average particle multiplicity in the transverse regions.

Since the particle multiplicity is sensitive to the details of the colour structure of the final state, the effect of chosing short or long string configurations is shown in Fig. 6. In the present simulation the long string configuration is preferred.

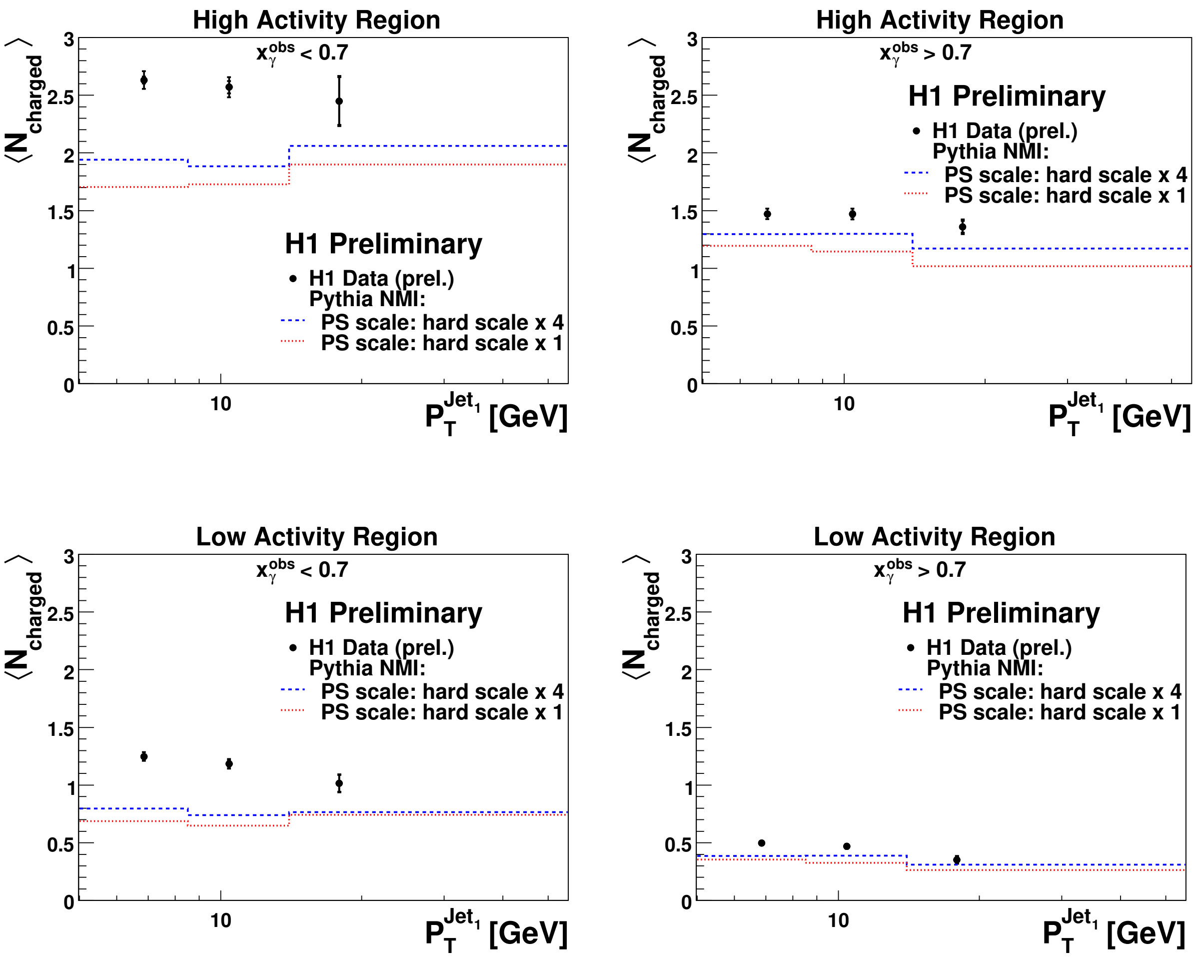

Figure 5: Charged particle multiplicity for $x_\gamma < 0.7$ (left) and for $x_\gamma > 0.7$ (right). The transverse high activity regions, upper plots, are defined as the transverse region with a higher E_t^{sum} compared to the low activity regions, down. The comparison of PYTHIA without MPI with an upper scale for the PS four times the hard scattering scale and with this scale set to the hard scattering is shown

4 Conclusion

The average charged particle multiplicity in photoproduction of dijet events has been measured as a function of the azimuthal angle with respect to the leading jet and compared to PYTHIA. The charged particle multiplicity has been investigated for two different regions in x_γ separating the point-like from the hadronic (resolved) photon and as a function of the leading jet transverse momentum. In the region of $x_\gamma > 0.7$ the charged particle multiplicity is reasonably well described by PYTHIA including one hard scattering process supplemented with parton showers and hadronisation but without MPI. The region of $x_\gamma < 0.7$ shows clearly, that the charged particle multiplicity is larger than what is expected from this simulation, and is well described when multi-parton interactions are included. The multi-parton interaction simulation describes the measurement better when the colour structure of the final state is chosen such that long

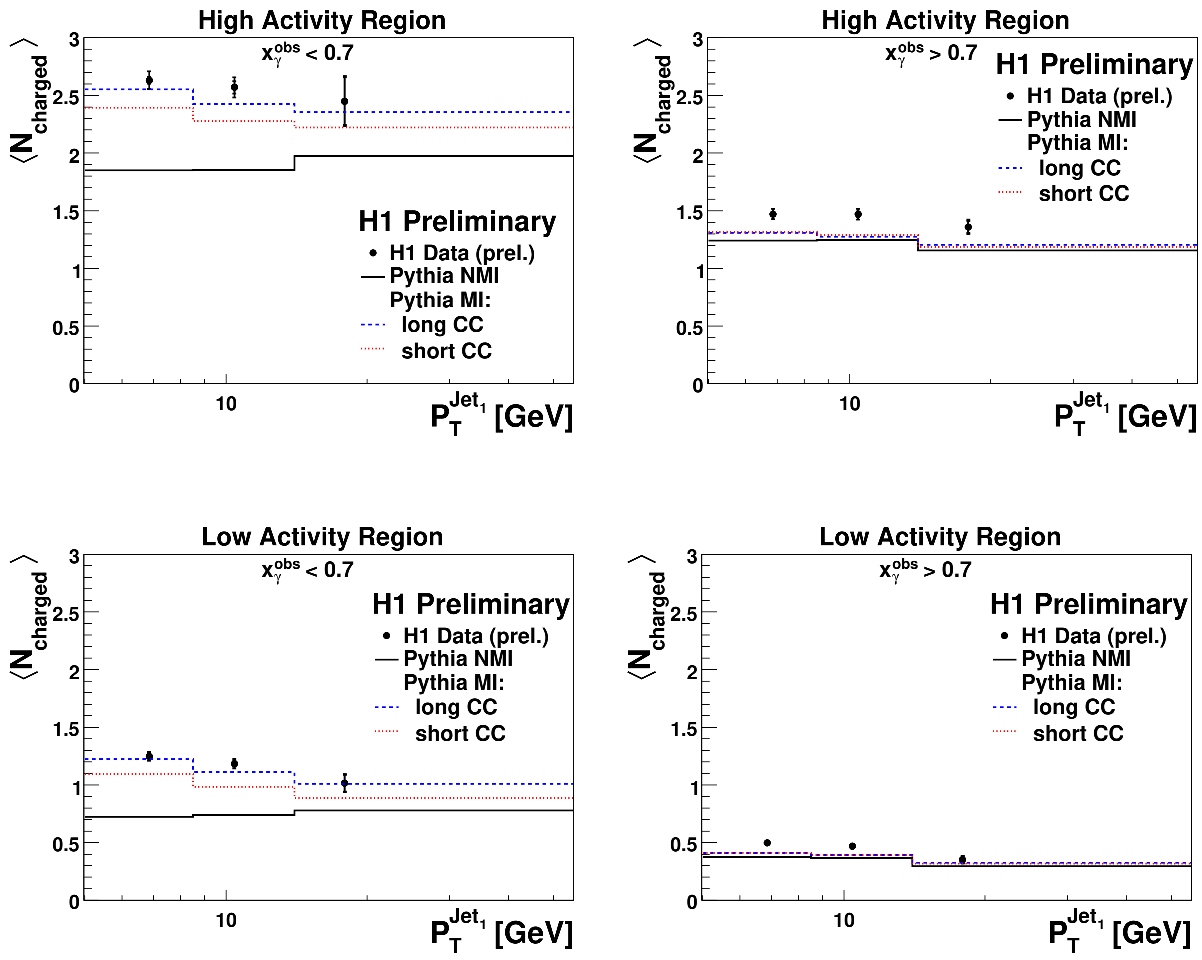

Figure 6: Charged particle multiplicity for $x_\gamma < 0.7$, left, and for $x_\gamma > 0.7$, right. The transverse high activity regions, upper plots, are defined as the transverse region with a higher E_t^{sum} compared to the low activity regions, down. Here data is compared to PYTHIA without MPI and PYTHIA with MPI and high probability for long colour string connections, long CC, and short colour string connections, short CC.

string lengths are preferred.

It was also shown, that the charged particle multiplicity in the transverse region cannot be accounted for by increasing the amount of initial and final state radiation.

In the region where the photon develops a hadronic structure the measurement supports the picture where multi-parton interactions occur, very similar to what has been observed at the TeVatron.

Acknowledgments

We are grateful to the HERA machine group whose outstanding efforts have made this experiment possible. We thank the engineers and technicians for their work in constructing and maintaining the H1 detector, our funding agencies for financial support, the DESY technical staff for continual assistance and the DESY directorate for support and for the hospitality which they extend to the non DESY members of the collaboration.

5 References

References

[1] T. Sjöstrand, L. Lonnblad and S. Mrenna, ”PYTHIA 6.2: Physics and manual”, (2001), hep-ph/0108264.

T. Sjöstrand, S. Mrenna and P. Skands, ”PYTHIA 6.4 Physics and Manual”, JHEP 0605:026,2006. (2006), hep-ph/0603175.

[2] T. Sjöstrand and M. van Zijl, ”A multiple-interaction model for the event structure in hadron collisions”, Phys. Rev. D36 (1987), 7, 2019–2041.

[3] S. Aid *et al.* [H1 Collaboration], ”Jets and Energy Flow in Photon-Proton Collisions at HERA”, Z. Phys. C 70 (1996) 17.

[4] T. Affolder, *et al.* [CDF Collaboration], ”Charged jet evolution and the underlying event in proton anti-proton collisions at 1.8-TeV”, Phys. Rev. D65 (2002) 092002.

[5] J. Pumplin, *et al.*, ”New generation of parton distributions with uncertainties from global QCD analysis”, JHEP **0207** (2002) 012 [arXiv:hep-ph/0201195].

[6] G. A. Schuler and T. Sjostrand, ”Parton Distributions of the Virtual Photon”, Phys. Lett. B **376** (1996) 193 [arXiv:hep-ph/9601282].

[7] D’Agostini, G., ”A Multidimensional unfolding method based on Bayes’ theorem”, Nucl. Instrum. Meth. A362 (1995), 487-498.